Paraorbital ground state of the trivalent Ni ion in $LiNiO_2$ from DFT+DMFT calculations

Dm. M. Korotin,[1,*] D. Novoselov,[1,2] and V. I. Anisimov[1,2]

[1]*M. N. Mikheev Institute of Metal Physics, S. Kovalevskoy St. 18, 620108 Yekaterinburg, Russia*

[2]*Institute of Physics and Technology, Ural Federal University, Mira St. 19, 620002 Yekaterinburg, Russia*

(Received 1 March 2018; revised manuscript received 29 November 2018; published 2 January 2019)

In $LiNiO_2$, the Ni^{3+} ion has a d^7 configuration in a cubic crystal field with one electron on doubly degenerate e_g orbitals, and such an ion is considered to be Jahn-Teller (JT) active. However, despite the fact that this compound is an insulator, and hence d-electrons are localized, a cooperative JT lattice distortion was not observed. This problem was usually supposed to be resolved by the presence of local JT distortions that do not order in a cooperative JT distorted crystal structure. In the present work, the DFT+DMFT approach, combining density functional theory with dynamical mean-field theory, was applied to study the electronic and magnetic properties of $LiNiO_2$. In the result, an insulating solution with a small energy gap value was obtained in agreement with experimental data. However, in contrast to previous calculations by other methods, the symmetry was not broken and the calculated ground state is a thermodynamical mixture of $\alpha d^7 + \beta d^8 L$ ($\alpha \approx 60\%$, $\beta \approx 40\%$) ionic states. The $d^8 L$ state is JT inactive, and we have found that for the nickel d^7 state two configurations with an electron on the Ni $d_{x^2-y^2}$ or $d_{3z^2-r^2}$ orbital have equal statistical weights. So the orbital degeneracy of the Ni^{3+} ion is not lifted, and that explains the absence of the cooperative JT lattice distortion in this compound. Also, the temperature dependence of inverse magnetic susceptibility of $LiNiO_2$ has been calculated, and a good agreement with experimental data was obtained.

DOI: 10.1103/PhysRevB.99.045106

I. INTRODUCTION

Starting from the paper of Goodenough *et al.* [1], it is accepted that in $LiNiO_2$ the Ni^{3+} ion in a d^7 configuration contains a single electron on doubly degenerate e_g orbitals set with filled t_{2g} orbitals. Correspondingly, the Ni^{3+} ion is in the low-spin magnetic state with $S = 1/2$.

The ground state of an isolated Ni^{3+} ion is fourfold degenerate: it has twofold orbital and twofold spin degeneracy. A standard scenario would be that the orbital degeneracy is resolved by a (cooperative) Jahn-Teller effect, while the spin degeneracy is lifted by magnetic ordering. Let us note that, as far as the e_g electrons are concerned, the cooperative Jahn-Teller effect is synonymous with orbital ordering. Thus it can be explained with a purely electronic model, without consideration of electron-lattice coupling.

$LiNiO_2$ does not undergo a Jahn-Teller distortion [2], and though the measured susceptibility shows some anomalies, it does not seem to develop magnetic long-range order [3,4]. So this compound presents a problem, where an insulator with a transition-metal ion in Jahn-Teller (JT) active configuration remains in the paraorbital and paramagnetic state until the lowest temperatures.

This problem was supposed to be resolved by the presence of local JT distortions that do not order in cooperative JT distorted crystal structure. Local JT distortions have been observed with extended and transmission x-ray-absorption fine structure (EXAFS and XAFS) experiments [2,5]. The absence of long-range JT distortion around the Ni^{3+} ion was explained with randomly oriented JT orbitals [2,6]; the formations of 10-nm-sized domains with orbital ordering and local JT distortion within, but with undistorted structure on average [7]; random distribution of the Ni^{2+} impurities within $LiNiO_2$ [8]; and charge disproportionation [9] of the Ni^{3+} cations into Ni^{2+} and Ni^{4+}. The problem of orbital-ordering and the presence of the JT effect in stoichiometric $LiNiO_2$ seems to be still open. Magnetic measurements show anomalous magnetic properties of $LiNiO_2$ at low temperatures but without long-range magnetic ordering (see, for example, [10] and Refs. [2–20] within). Magnetic susceptibility corresponds to a system of $S = 1/2$ spins with weak ferromagnetic coupling [3].

An electronic-structure calculation for $LiNiO_2$ within density functional theory (DFT) results in a metallic ground state that contradicts the experimentally observed insulating state with a small energy gap (0.5 eV in [11], $\approx$0.4 eV in [12], and $\geqslant$0.1 eV in [13]). This contradiction is an indication of electronic state localization and the importance of electronic Coulomb correlations. If one takes into account the correlations within the DFT+U approach, then an insulator solution could be obtained [12], but the DFT+U method assumes long-range magnetic and orbital order while an experimentally paramagnetic and paraorbital state is observed until the lowest temperatures in $LiNiO_2$.

The DFT+U method corresponds to the static mean-field approximation for the Coulomb interaction Hamiltonian [12,14]. This means that its solution corresponds to the ground state in the form of a single Slater determinant with fixed spin-orbital occupancy values, which breaks symmetry and imposes orbital and spin order on the system. Previously published results of calculations within DFT+U indicates that a low-symmetry JT-distorted structure is the lowest one for

*dmitry@korotin.name

$LiNiO_2$ [15,16]. However, one can use the dynamical mean-field theory (DMFT) [17–19] approach and obtain the ground state as a thermodynamical mixture of various electronic configurations (Slater determinants). The statistical weights of the contributing configurations to the ground state could be computed directly. In the result, one obtains a Green function that describes ground-state and excitation spectra for the system under consideration, without breaking symmetry and imposing unnecessary spin and orbital order. Hence it is possible to obtain an insulating solution for one electron in an e_g band preserving a high-symmetry paraorbital and paramagnetic state. This was demonstrated on a model level in [20].

In the present work, we have used the *ab initio* DFT+DMFT approach, combining density functional theory with dynamical mean-field theory [21], to calculate the electronic structure and the spectral and magnetic properties of $LiNiO_2$. Since such calculations are time- and resource-consuming, it was useful to find a minimally sufficient model for the electronic and magnetic properties description of $LiNiO_2$. We used three effective noninteracting Hamiltonians in the basis of Wannier functions, constructed as a postprocessing step of DFT calculation of the compound. The first Hamiltonian corresponds to a minimal model in the basis of two Wannier functions, corresponding to the partially filled e_g band. Since it is conventional that the Ni^{3+} ion could not be in d^n but in a $d^{n+1}L$ configuration, the second Hamiltonian includes in addition oxygen states and takes into account O-$2p$ and partially filled Ni-e_g state hybridization effects in $LiNiO_2$. The third (the most complex $d+p$) Hamiltonian included Ni e_g, Ni t_{2g}, and O p-states. The analysis of the calculated two-band Hamiltonian parameters indicates that the triangular lattice models with nearest-neighbor hopping only, used in the literature [22,23] for the $LiNiO_2$ magnetic and orbital orderings description, are oversimplified. The calculated intersite electron transfer energies for the Ni ions are rather long-ranged, which was ignored earlier. In the result of DFT+DMFT calculations for the constructed Hamiltonians, we have obtained a small-gap insulator in the paramagnetic and paraorbital state, in agreement with experimental data. The nickel ions are in the mixed $\alpha d^7 + \beta d^8 L$ configuration where the statistical weight of the d^7 state is 56% for the $e_g + p$ model and 48% for the $d + p$ model; the weight of the $d^8 L$ state is 40%/46% for the mentioned models, and there is also about 4%/5% of the $d^9 L^2$ configuration at 232 K. The Ni $d^8 L$ state does not assume the appearance JT distortion. Within the d^7 state, the statistical weight of the configuration with a filled Ni $d_{x^2-y^2}$ orbital equals the weight of the configuration with a filled Ni $d_{3z^2-r^2}$ orbital. Therefore, in the obtained solution there are no prerequisites for the JT distortion to arise in $LiNiO_2$. We have also calculated the temperature dependence of the magnetic susceptibility, which agrees well with experiment.

II. METHODS

In this work, we have used the DFT+DMFT calculation procedure described in [24]. The DFT calculation was done with the QUANTUM ESPRESSO [25] package, the Perdue-Burke-Ernzerhof (PBE) exchange-correlation functional, a regular $16 \times 16 \times 16$ k-points mesh in the irreducible part of the Brillouin zone for reciprocal space integrals, and energy cutoff values equal to 45 and 450 Ry for wave functions and charge density, respectively. The lattice parameters for space group R-$3m$ were taken as $a = 2.833$ Å and $c = 14.215$ Å [26].

In the crystal field of the ligand octahedron, the Ni-d energy bands are split into a filled t_{2g} subband and a partially filled e_g subband with the one electron. The band structure of $LiNiO_2$ calculated within DFT is presented in Fig. 1(a). The Fermi level crosses two partially filled e_g^σ energy bands that are separated from the fully occupied low-energy states formed by O $2p$ and Ni $3d$ t_{2g}.

We used the three different basis sets for the model Hamiltonians to consider the Coulomb correlations in $LiNiO_2$. The first one is a minimal basis of two Wannier functions (WFs) with the symmetry of Ni e_g orbitals. The WFs were constructed by a projection of Bloch functions with energies in the interval $[-1; 1]$ eV around the Fermi level on the atomic wave functions centered on the Ni ions and having a symmetry of Ni e_g orbitals (the projection routine is described in detail in [24]). We did not perform an additional localization procedure here, striving to keep the symmetry of WF unchanged. The energy bands of the resulting model Hamiltonian and spatial distribution of the basis WFs are shown in Figs. 1(a) and 1(b).

Since there is a significant hybridization between nickel and oxygen states in $LiNiO_2$, the two partially filled energy bands, which cross the Fermi level, are formed by a mixture of the Ni-d and O-p orbitals. The Wannier functions of the minimal basis [Fig. 1(b)], describing the partially filled energy bands, are centered on the Ni ion and have a substantial contribution from the p-states of the neighboring oxygen ions. Each WF could be presented as a sum of atomic orbitals $|\phi_{m,n}\rangle$ $(n = s, p, d, \dots)$ of the neighboring atoms m, and in the specific case as a sum of Ni-d and the p states of the nearest oxygen ions. Contributions from the other states (Ni-s, O-s, etc) are negligible,

$$|\mathrm{WF}\rangle = \sum_{n,m} c_{m,n}|\phi_{m,n}\rangle = \sum_{n=d,m=Ni} a_n|\phi_{m,n}\rangle + \sum_{n=p,m=O} b_n|\phi_{m,n}\rangle. \quad (1)$$

For the minimal basis set describing only two energy bands, we estimated each Wannier function's composition ($c_{m,n} = \langle\phi_{m,n}|\mathrm{WF}\rangle$) as 55% of Ni-$e_g$ and 45% of the nearest O-p states.

To consider the charge-transfer effect, we build the second model noninteracting Hamiltonian in an extended basis set that includes Ni-e_g states as well as O-p states hybridized with the former by symmetry. Wishing to keep the number of Wannier functions as small as possible, we took into account only oxygen states that are mostly hybridized with the Ni ones. The Bloch functions with energies in the full interval $[-7; 1]$ eV were projected on a trial wave functions constructed as $|\tilde{\phi}_d\rangle = \sum_{n=d,m=Ni} a_n|\phi_{m,n}\rangle$ and $|\tilde{\phi}_p\rangle = \sum_{n=p,m=O} b_n|\phi_{m,n}\rangle$, where coefficients a_n and b_n were set the same as for the first basis-set Wannier functions. The resulting four WFs (two WF of Ni-e_g + two WFs of O-p) and the model noninteracting Hamiltonian band structure are presented in Figs. 1(c) and 1(d). Since there was no localization or disentanglement

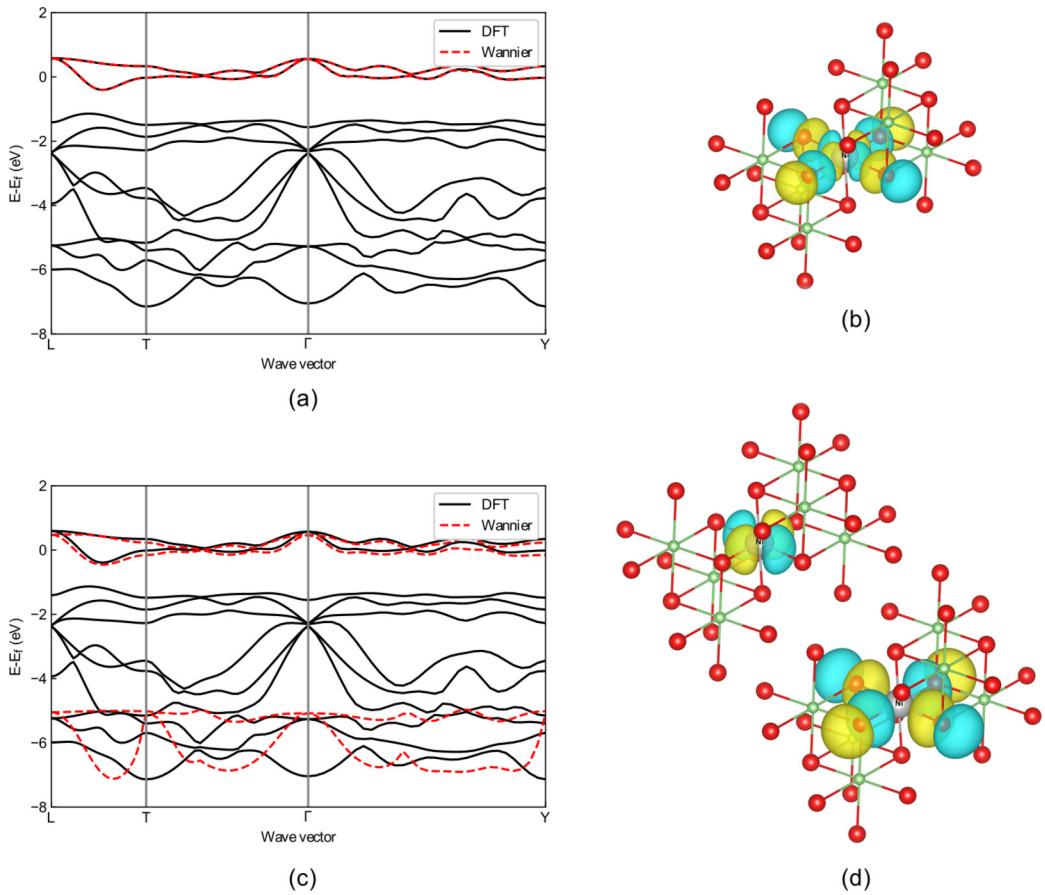

FIG. 1. (a) Calculated DFT band structure of $LiNiO_2$ (black solid line) and bands obtained from the noninteracting Hamiltonian in the minimal Wannier functions basis (red dashed line). (b) Corresponding WF with the symmetry of the Ni-$d_{x^2-y^2}$ orbital. (c) The DFT (black solid line) and the noninteracting Hamiltonian (red dashed line) band structure of $LiNiO_2$ for the second basis set, which directly includes oxygen p-states hybridized with Ni-e_g. (d) The resulting Ni-$d_{x^2-y^2}$ and O-p WFs. The two additional basis WFs (Ni-$d_{3z^2-r^2}$ and another O-p) are not shown. Red spheres denote oxygen ions; green ones, Li ions.

procedure applied for the oxygen WFs, the resulting model oxygen bands do not coincide with the DFT ones exactly. Nevertheless, the bands' centers and the O-p Ni-e_g energy levels splitting, the value of which is responsible for d^8L state formation, are finely reproduced within this model.

As the third noninteracting starting Hamiltonian, we considered a model with 11 WFs as a basis set: Ni-t_{2g}, Ni-e_g, and O-p (for both oxygen ions in the crystal cell). The energy window used in projection procedure $[-7; 1]$ eV contains 11 DFT energy bands that are well reproduced with the resulting model Hamiltonian.

The noninteracting Hamiltonians in the three basis sets were used as input for the DMFT calculation performed within the AMULET package [27]. Since the Hubbard U parameter depends strongly on WF spatial distribution and a more localized basis assumes a larger Coulomb interaction strength [28], the U value for the minimal basis (2 WFs of Ni e_g-symmetry) was set to $U = 4.0$ eV [29] (see Fig. 2). As for the second basis set (2 WF of Ni-e_g + 2 WFs of O-p) and the third one (5 Ni-d + 2 O-p), we used $U = 8.0$ eV. The Hund exchange parameter $J = 0.9$ eV was used in all cases. For the largest model Hamiltonian, we included intersite Coulomb interaction (V) in the consideration as described in [30] with $V = 2.0$ eV. To solve the impurity problem, we used the

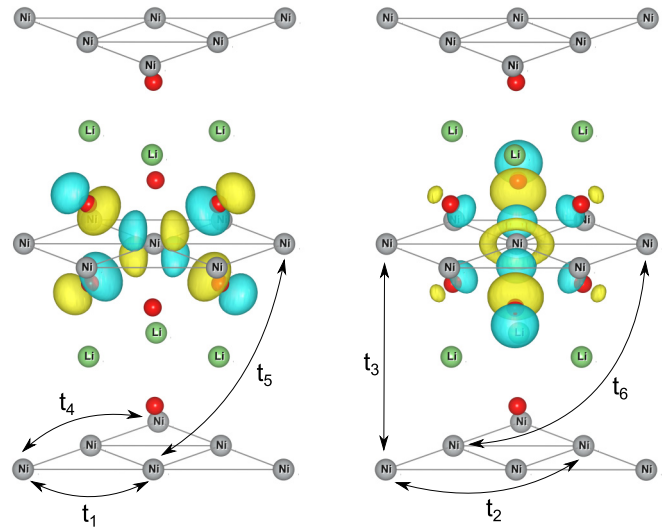

FIG. 2. The spatial distribution of Wannier functions with symmetry of the Ni $d_{x^2-y^2}$ orbital (left panel) and the $d_{3z^2-r^2}$ orbital (right panel). The Ni ions are denoted with gray balls, the O ions with red balls, and the Li ion with green balls. The directions of the nearest-neighboring hopping integrals t_1–t_6 are shown with arrows.

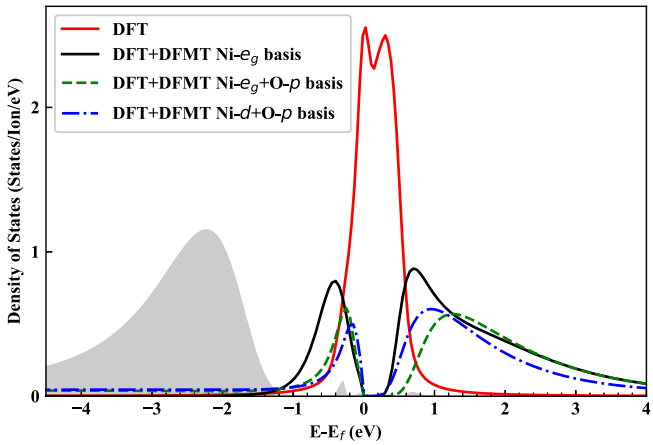

FIG. 3. Calculated density of states for e_g electrons of $LiNiO_2$. Red solid line, DOS obtained within DFT calculation; black solid line, DOS calculated within the DFT+DMFT approach in the minimal basis of two WFs; green dashed line, DOS calculated within the DFT+DMFT approach in the basis of Ni-e_g + O-p WFs; blue dot-dashed line, DOS calculated within the DFT+DMFT approach in the full basis of Ni-d + O-p WFs. The gray filled area corresponds to Ni-t_{2g} DOS obtained in the last model.

continuous-time quantum Monte-Carlo algorithm (CT-QMC) [31]. For the spectral function calculation (Fig. 3), in the QMC [32] simulations, the inverse temperature value was up to $\beta = 50\,\mathrm{eV}^{-1}$ and we used (1.5×10^6)–(9×10^6) Monte Carlo sweeps.

For the minimal basis set, the calculated kinetic energy of an electron transfer for WF of one Ni site to WF of the neighboring Ni site (i.e., the hopping integral of the effective model Hamiltonian) is long-range, as shown in Table I. The hopping parameters to the fourth nearest Ni neighbor are more significant than the hoppings to the first three nearest neighbors. This happens due to an overlap of the neighboring ion WFs on the oxygen sites in between, because of the large contribution to WF from O-p orbitals. The significant values for the hopping integrals between the Ni planes (t_5 and t_6) indicate that if one tries to construct a triangular lattice model for a magnetic properties description of $LiNiO_2$ as in [22,33,34], the interlayer Ni-Ni exchange interaction should not be neglected. On the other hand, in the extended Ni-e_g + O-p basis, the direct Ni-Ni hoppings decrease with distance, and even for the second nearest neighbor they do not exceed 50 eV (see Table I). However, in this case, the Ni-O electron transfer should be included in any used model.

III. RESULTS AND DISCUSSION

The density of states of the nickel e_g electrons in $LiNiO_2$ calculated within the DFT+DMFT approach for a temperature of 232 K is presented in Fig. 3. We have obtained an insulating solution with the energy gap value from 0.3 (the minimal and the full basis) to 0.45 eV (the second basis set), which is in agreement with experimental values 0.4–0.5 eV [11,12]. The used method does not enforce any long-range magnetic or orbital ordering, and the obtained solution is paramagnetic and paraorbital. The obtained mean value for the total magnetization operator $\langle s_z \rangle$ is zero in the whole used temperature range 232–1160 K, therefore there is no evidence of magnetic ordering.

The hybridization expansion CT-QMC solver provides the site-reduced statistical operator (density matrix) [35]. This quantity describes the probability of finding an atom in a particular many-body state, and an expectation value of any local operator can be easily obtained from it. Therefore, this instrument is well suited to analyze the statistical probability of the various atomic configurations of the Ni ion.

In the calculated ground state, the two Ni $d_{x^2-y^2}$ and $d_{3z^2-r^2}$ orbitals are equally filled and the corresponding configurations have the same statistical weights. In the minimal basis of two WFs, each Wannier function is filled with 0.5 electrons in a mean or is totally filled with a probability of 50%. The second, extended basis of Ni-e_g and O-p WFs, gives a more complex result. Due to the charge-transfer effect taken into account, the configuration d^8L with the totally filled e_g subshell has a statistical weight equal to 40%. This electronic configuration is Jahn-Teller inactive. The d^7 configuration has a weight of 56% and d^9L^2 takes the remaining 4%. Even for the second basis, the WFs of Ni-e_g symmetry have an equal occupation number and the same statistical weight. The solution for the largest $d + p$ model gives qualitatively the same result with a slightly different distribution of the population probabilities of Ni ion electronic configurations: 48% for d^7, 46% for d^8L, and 5% for d^9L^2. Consequently, on average, both e_g orbitals are degenerate and are filled equivalently, therefore there are no preconditions for the appearance of the Jahn-Teller lattice distortion.

To study the magnetic properties of $LiNiO_2$, the temperature dependence of magnetic susceptibility has been calculated in the DFT+DMFT method. It was done by applying a small magnetic field on Ni ions and calculating the resulting spin polarization. The ratio of the polarization value to the magnetic-field value is susceptibility. The result is shown in Fig. 4. From the $\chi^{-1}(T)$ dependence, the effective magnetic moment of the Ni ion and the Curie-Weiss parameter θ were

TABLE I. Calculated kinetic energy (meV) of an electron transfer t_n^{ij} for the ith e_g-like WF of one Ni site to the jth e_g-like WF of the neighboring Ni site. The electron hopping directions t_n are shown in Fig. 2.

Basis	$t_1^{i,j}$	$t_2^{i,j}$	$t_3^{i,j}$	$t_4^{i,j}$	$t_5^{i,j}$	$t_6^{i,j}$
Ni-e_g	$\begin{pmatrix} 47 & 0 \\ 0 & -16 \end{pmatrix}$	$\begin{pmatrix} 10 & -6 \\ -6 & 4 \end{pmatrix}$	$\begin{pmatrix} -1 & 0 \\ 0 & 9 \end{pmatrix}$	$\begin{pmatrix} 17 & -42 \\ -42 & 66 \end{pmatrix}$	$\begin{pmatrix} 49 & 0 \\ 0 & -19 \end{pmatrix}$	$\begin{pmatrix} -23 & -13 \\ -13 & -10 \end{pmatrix}$
Ni-e_g + O-p	$\begin{pmatrix} 42 & 0 \\ 0 & -66 \end{pmatrix}$	$\begin{pmatrix} 17 & -16 \\ -16 & -1 \end{pmatrix}$	$\begin{pmatrix} 20 & 0 \\ 0 & -15 \end{pmatrix}$	$\begin{pmatrix} 12 & 10 \\ 10 & 0 \end{pmatrix}$	$\begin{pmatrix} -16 & 0 \\ 0 & -10 \end{pmatrix}$	$\begin{pmatrix} -3 & -6 \\ -6 & 14 \end{pmatrix}$

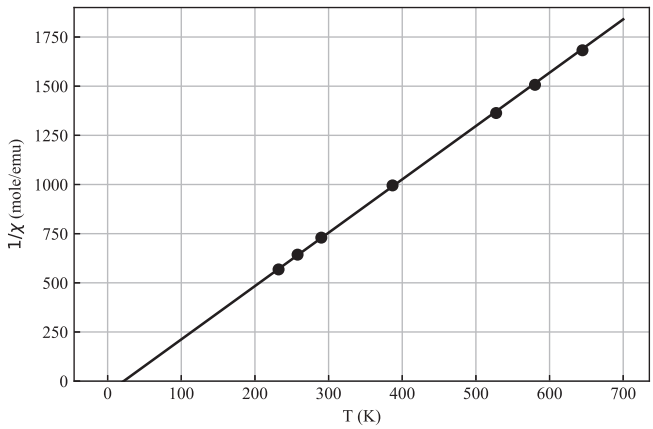

FIG. 4. Calculated inverse magnetic susceptibility for $LiNiO_2$. The black dots denote calculated values; the black solid line is plotted using the least-squares approximation method.

calculated. The calculated value of $\mu_{\text{eff}} = 1.22/1.4\mu_B$ (for the models without and with oxygen states) is slightly underestimated compared with with experimental values for the effective moment ($1.91\mu_B$ [3] and $2.1\mu_B$ [36–38]) but both correspond to the formal spin state $S = 1/2$. The calculated Curie-Weiss parameter $\theta = 22$ K is in good agreement with experimental values θ (19 K [39], 26 K [38], 29 K [37], and 41 K [36]). The positive sign of calculated θ confirms the weak ferromagnetic coupling between $S = 1/2$ spins in $LiNiO_2$.

A comparison of the results obtained for the three models used demonstrates that such physical properties as the atomic magnetic moment and the energy gap value are close to each other in all three cases. We conclude that the minimally sufficient model for $LiNiO_2$ is the one with only two Ni-e_g states considered as Hamiltonian basis functions.

IV. CONCLUSION

In DFT+DMFT calculations, we have obtained the paramagnetic paraorbital insulating ground state for $LiNiO_2$. The obtained ground state is the mixture of d^7, d^8L, and less than 5% of d^9L^2 configurations of the Ni ion. The two e_g orbitals have the same average occupancy in all these configurations, therefore even within the d^7 configuration a prerequisite of Jahn-Teller distortion of the ligands octahedron is absent. Within the same approach, the magnetic susceptibility dependence on temperature has been computed. Calculated Curie-Weiss parameters μ_{eff} and θ are in agreement with available experimental data.

ACKNOWLEDGMENTS

The temperature dependence of inverse magnetic susceptibility for $LiNiO_2$ was obtained within the state assignment of FASO of Russia (theme "Electron" No. AAAA-A18-118020190098-5). The spectral functions were calculated within the RSF grant (Project 14-22-00004). D.K. is grateful to A. I. Poteryaev for valuable discussions.

[1] J. B. Goodenough, D. G. Wickham, and W. J. Croft, J. Phys. Chem. Solids **5**, 107 (1958).
[2] A. Rougier, C. Delmas, and A. V. Chadwick, Solid State Commun. **94**, 123 (1995).
[3] K. Yamaura, M. Takano, A. Hirano, and R. Kanno, J. Solid State Chem. **127**, 109 (1996).
[4] K. Hirota, Y. Nakazawa, and M. Ishikawa, J. Phys.: Condens. Matter **3**, 4721 (1991).
[5] I. Nakai, K. Takahashi, Y. Shiraishi, T. Nakagome, and F. Nishikawa, J. Solid State Chem. **140**, 145 (1998).
[6] C. Pouillerie, E. Suard, and C. Delmas, J. Solid State Chem. **158**, 187 (2001).
[7] J.-H. Chung, T. Proffen, S. Shamoto, A. M. Ghorayeb, L. Croguennec, W. Tian, B. C. Sales, R. Jin, D. Mandrus, and T. Egami, Phys. Rev. B **71**, 064410 (2005).
[8] L. Petit, G. M. Stocks, T. Egami, Z. Szotek, and W. M. Temmerman, Phys. Rev. Lett. **97**, 146405 (2006).
[9] H. Chen, C. L. Freeman, and J. H. Harding, Phys. Rev. B **84**, 085108 (2011).
[10] F. Reynaud, D. Mertz, F. Celestini, J. M. Debierre, A. M. Ghorayeb, P. Simon, A. Stepanov, J. Voiron, and C. Delmas, Phys. Rev. Lett. **86**, 3638 (2001).
[11] J. Molenda, P. Wilk, and J. Marzec, Solid State Ion. **146**, 73 (2002).
[12] V. I. Anisimov, J. Zaanen, and O. K. Andersen, Phys. Rev. B **44**, 943 (1991).
[13] V. R. Galakhov, E. Z. Kurmaev, S. Uhlenbrock, M. Neumann, D. G. Kellerman, and V. S. Gorshkov, Solid State Commun. **95**, 347 (1995).
[14] V. I. Anisimov, F. Aryasetiawan, and A. I. Lichtenstein, J. Phys.: Condens. Matter **9**, 767 (1997).
[15] Z. Chen, H. Zou, X. Zhu, J. Zou, and J. Cao, J. Solid State Chem. **184**, 1784 (2011).
[16] H. Chen and J. H. Harding, Phys. Rev. B **85**, 115127 (2012).
[17] W. Metzner and D. Vollhardt, Phys. Rev. Lett. **62**, 324 (1989).
[18] A. Georges, G. Kotliar, W. Krauth, and M. J. Rozenberg, Rev. Mod. Phys. **68**, 13 (1996).
[19] G. Kotliar, S. Y. Savrasov, K. Haule, V. S. Oudovenko, O. Parcollet, and C. A. Marianetti, Rev. Mod. Phys. **78**, 865 (2006).
[20] A. I. Poteryaev, M. Ferrero, A. Georges, and O. Parcollet, Phys. Rev. B **78**, 045115 (2008).
[21] V. I. Anisimov, A. I. Poteryaev, M. A. Korotin, A. O. Anokhin, G. Kotliar, U. K. Pii, and M. Physics, J. Phys.: Condens. Matter **9**, 7359 (1997).
[22] M. V. Mostovoy and D. I. Khomskii, Phys. Rev. Lett. **89**, 227203 (2002).
[23] F. Vernay, K. Penc, P. Fazekas, and F. Mila, Phys. Rev. B **70**, 014428 (2004).
[24] D. Korotin, A. V. Kozhevnikov, S. L. Skornyakov, I. Leonov, N. Binggeli, V. I. Anisimov, and G. Trimarchi, Eur. Phys. J. B **65**, 91 (2008).

[25] P. Giannozzi, S. Baroni, N. Bonini, M. Calandra, R. Car, C. Cavazzoni, D. Ceresoli, G. L. Chiarotti, M. Cococcioni, I. Dabo, A. Dal Corso, S. de Gironcoli, S. Fabris, G. Fratesi, R. Gebauer, U. Gerstmann, C. Gougoussis, A. Kokalj, M. Lazzeri, L. Martin-Samos, N. Marzari, F. Mauri, R. Mazzarello, S. Paolini, A. Pasquarello, L. Paulatto, C. Sbraccia, S. Scandolo, G. Sclauzero, A. P. Seitsonen, A. Smogunov, P. Umari, and R. M. Wentzcovitch, J. Phys.: Condens. Matter **21**, 395502 (2009).

[26] W. Li, J. Reimers, and J. Dahn, Solid State Ion. **67**, 123 (1993).

[27] AMULET code: http://amulet-code.org.

[28] V. I. Anisimov, Dm. M. Korotin, S. V. Streltsov, A. V. Kozhevnikov, J. Kuneš, A. O. Shorikov, and M. A. Korotin, JETP Lett. **88**, 729 (2008).

[29] S. Laubach, S. Laubach, P. C. Schmidt, D. Ensling, S. Schmid, W. Jaegermann, A. Thißen, K. Nikolowski, and H. Ehrenberg, Phys. Chem. Chem. Phys. **11**, 3278 (2009).

[30] A. S. Belozerov, M. A. Korotin, V. I. Anisimov, and A. I. Poteryaev, Phys. Rev. B **85**, 045109 (2012).

[31] E. Gull, A. J. Millis, A. I. Lichtenstein, A. N. Rubtsov, M. Troyer, and P. Werner, Rev. Mod. Phys. **83**, 349 (2011).

[32] J. E. Hirsch and R. M. Fye, Phys. Rev. Lett. **56**, 2521 (1986).

[33] Y. Q. Li, M. Ma, D. N. Shi, and F. C. Zhang, Phys. Rev. Lett. **81**, 3527 (1998).

[34] K. Hirota, H. Yoshizawa, and M. Ishikawa, J. Phys.: Condens. Matter **4**, 6291 (1992).

[35] P. Werner and A. J. Millis, Phys. Rev. Lett. **99**, 126405 (2007).

[36] J. Sugiyama, Y. Ikedo, K. Mukai, H. Nozaki, M. Månsson, O. Ofer, M. Harada, K. Kamazawa, Y. Miyake, J. H. Brewer, E. J. Ansaldo, K. H. Chow, I. Watanabe, and T. Ohzuku, Phys. Rev. B **82**, 224412 (2010).

[37] M. Bonda, M. Holzapfel, S. de Brion, C. Darie, T. Fehér, P. J. Baker, T. Lancaster, S. J. Blundell, and F. L. Pratt, Phys. Rev. B **78**, 104409 (2008).

[38] J. N. Reimers, J. Dahn, J. Greedan, C. Stager, G. Liu, I. Davidson, and U. Von Sacken, J. Solid State Chem. **102**, 542 (1993).

[39] F. Reynaud, A. M. Ghorayeb, Y. Ksari, N. Menguy, A. Stepanov, and C. Delmas, Eur. Phys. J. B **14**, 83 (2000).